Acta Neuropathol (1992) 85: 55 – 70

Acta Neuropathologica

Ibotenic acid-induced calcium deposits in rat substantia nigra

Ultrastructure of their time-dependent formation*

Cordula Nitsch and Alessandra L. Scotti

Section of Neuroanatomy, Institute of Anatomy, University of Basel, Pestalozzistrasse 20, CH-4056 Basel, Switzerland

Received May 11, 1992/Revised, accepted June 30, 1992

Summary. The excitotoxin ibotenic acid (IBO) induces local calcium deposits upon injection into rat substantia nigra. Their formation has been investigated at the ultrastructural level in a time course study from 2 days to 8 weeks survival. Potassium bichromate stain was used to visualize pathological calcium accumulation. Two days after IBO application, reaction product for calcium was observed in mitochondria of degenerating perikarya and dendrites, but not in axons, boutons or glia. Four days after the lesion, calcium stain was found, in addition, in a seemingly free form in a few dendrites, especially those still contacted by intact boutons and not sequestrated by invading glia. Two days later, most of these calcium-accumulating dendrites were separated by astroglia from their synaptic partners. At the border between glia and dendrite a fibrillar matrix was formed which further accumulated calcium. During the following weeks this matrix enlarged stepwise and was infiltrated with calcium, thus giving a picture resembling the annual growth rings of trees. The evolving bodies incorporated smaller deposits in their vicinity, finally representing the large concretions seen at the light microscopic level from the 4th postoperative week onward. Similarities and dissimilarities of these observations with the results from other ultrastructural studies on excitotoxin lesions are detailed. It is suggested that the different outfit of neuronal subpopulations and of glia with ligand-gated and metabotropic glutamate receptors in the single brain region, as well as the local response repertoire of glial cells towards the excitotoxic injury with the subsequent formation of a calcium-accumulating matrix provide the molecular basis for the formation of calcium deposits.

Key words: Excitotoxin – Substantia nigra – Neuronal degeneration – Calcification – Rat

Ibotenic acid (IBO), a conformationally restricted analog of the excitatory amino acid glutamate, is widely used to place locally circumscript axon-sparing brain lesions. The neurotoxic potential of IBO as well as of the previously identified kainic acid (KA) [7] is due to the affinity of these substances to the glutamate receptor. IBO is preferred to KA in lesion studies as it does not produce distant brain damage [18, 41]. The different effects are most probably caused by the different properties of the glutamate receptor subtypes to which these substances bind. IBO has an affinity for the *N*-methyl-D-aspartate (NMDA) type of receptor [23, 51] which gates a ligand-operated Ca^{2+} channel [22]. The Ca^{2+} influx generated upo IBO binding is thought to play a pivotal role in the cascade leading to nerve cell death [19]. The IBO-induced neuronal degeneration, thus, imitates the events considered to be responsible for nerve cell death in ischemia, epilepsy and possibly other neurodegenerative disorders [38].

In the course of our investigations on the long-term effects of different lesions in the striato-nigro-thalamic loop [30] we applied IBO to rat substantia nigra (SN) pars reticulata. Upon routine histological control of the lesion site 4 months after treatment, in the former SN basophilic concentric bodies were found which reached a diameter of up to 50 μm. They resembled calcium concretions, which was, in fact, verified histochemically [28, 29]. Subsequent studies revealed that the calcium deposits were specific to the SN, and that they could not be elicited in the caudate-putamen (CP) complex in the same form or frequency. The development of the deposits was time dependent and partially concentration dependent [28].

The ultrastructural appearance of the mature concretions has been shown in a preliminary communication [29]. In the present study it was our aim to elucidate in

* Dedicated to Professor Dr. K. S. Ludwig on the occasion of this 70th birthday. Supported in part by the Swiss Nationalfonds (No. 31-25292.88)

Correspondence to: C. Nitsch (address see above)

which tissue element(s) – neuronal or glial – the calcium accumulation originated and to investigate the process by which the deposits developed into the large masses visible in the light microscope.

Material and methods

Male Wistar rats (n = 11) 280–310 g in weight were used. Under chloralhydrate (0.4 g/kg i.p.) or pentobarbital (0.06 g/kg i.p.) anesthesia, they were fixed in a stereotaxic apparatus. IBO (Sigma, 14 µg in 0.7 µl buffered saline) was injected with a Hamilton microsyringe at the coordinates AP + 2.8 mm, L 2 mm and V 2 mm below ear zero plane according to the atlas of Pellegrino et al. [35]. Injection time was 10 min, and further 10 min elapsed before the needle was withdrawn and the wound closed. After the effects of anesthesia had subsided, the rats showed a marked tendency to rotate to the side contralateral to the injection [30]; a behavior which correlates which the exact localization of the excitotoxin injection.

After the survival times of 2 days (n = 2), 4 days (n = 1), 6 days (n = 2), 14 days (n = 1), 4 weeks (n = 2) and 8 weeks (n = 3), rats were reanesthetized and perfused transcardially with 4% paraformaldehyde and 0.2% glutaraldehyde in 0.1 M phosphate buffer, pH 7.4. The dissected brains were immersed in fixative overnight, and serial sagittal sections, 50 µm thick, were cut with a vibratome.

Alternating sections of the midbrain were further processed for:

1. Histological control of needle position and extent of nerve cell loss: mounting on slides, defatting, staining with 2% cresyl violet, dehydration, coverslipping with Eukitt
2. Light microscopic verification of calcium accumulation: mounting on slides, staining with Alizarin red (1% in 0.028% NH_4OH, pH 6.4) for 2 to 4 min and differentiation in acidified 96% ethanol [39], dehydration, coverslipping with Eukitt
3. Routine electron microscopy to study effect of lesion: postfixation in 0.1% OsO_4 in 0.9% NaCl for 1 h, blockstaining in 2% uranyl acetate in 70% ethanol for 1 h, dehydration in graded ethanol and propylenoxide, flat-embedding in Epon
4. Visualization of calcium accumulation at the ultrastructural level according to the method of Probst [37]: postfixation and staining in 1% OsO_4 and 2.5% $K_2Cr_2O_7$ for 1 h, continued as under 3
5. Control of the specificity of the potassium bichromate stain: pretreatment with 10 mM EGTA overnight, continued as under 4.

Light microscopy analysis was carried out with a Zeiss Axiophot. For the ultrastructural studies, ultrathin sections were obtained from the first 5 µm of the embedded vibratome slices. They were treated with lead citrate and viewed at in a Zeiss 10 electron microscope.

Results

Light microscopic observations

During the short survival periods of up to 14 days, the histological aspect of the IBO-induced lesion in the SN did not differ from that described in the literature (e.g., [40, 49]). A small globular necrotic center, where the needle tip had been positioned and in which all tissue elements were destroyed, was surrounded by a large zone of nerve cell loss. With optimal positioning of the injection in the center of the SN, the major part of this nucleus was destroyed from AP +4.4 to +2.8, and L: 1.4 to 2.9 according to the atlas of Paxinos and Watson [34] (see Fig. 1a, c, e). Damage to neighboring nuclei was minimal. Neuronal perikarya of both the SN pars compacta and the SN pars reticulata (Fig. 2a) were equally affected. Neurons were not detectable with the cresyl stain in animals with survival times of longer than 2 days. Gliosis became prominent 4 days after induction of the lesion (Fig. 1a) and was maximal 6 days post lesion (Figs. 1c, 2b).

After 4 weeks, apparently in a random distribution, basophilic calcium deposits were found across the whole extent of the neuron-depleted SN (Figs. 1e, 2e), with the exception of the immediate vicinity of the needle tip [29]. They varied in size between 5 and 25 µm. The number and size of calcium concretions increased over the following weeks (Fig. 2g), while gliosis subsided.

With an improved Alizarin red stain, as compared to our previous reports, we were now able to observe the first indication for calcium accumulation in the lesioned SN 4 days after IBO application (Figs. 1b, 2c). It was seen in the form of an amorphous to dust-like stain which in rare cases seemed to be concentrated in a few cells which could still be recognized as neurons. They were located at the outer perimeter of the SN. Six days after IBO application the Alizarin stain was found over the whole of the SN with the exception of the injection center (Fig. 1d). Occasionally the impression arose that the single dust-like particles concentrated to larger deposits (Fig. 2d). During the following weeks the grains further accumulated around the enlarging concretions, filling the whole extent of the SN, while leaving Alizarin-free areas in between (Figs. 1f, 2f). Eight weeks after IBO injection the mature calcium concretions had developed with their onion-shaped layered structure (Fig. 2h). These typical calcific bodies were mostly of ovoid to round shape, but occasionally were multilobulated and appeared to expand similar to a growing cauliflower.

Electron microscopic observations

Injection of the excitotoxin IBO elicited in the SN basically the same characteristic features of axon-sparing nerve cell degeneration, at least for the early survival periods up to 4 to 6 days, as described for comparable excitotoxic lesions. Perikarya of degenerated neurons could be recognized as such up to 4 days survival. Degeneration was characterized by clumping of chromatin and disintegration with later loss of nuclear envelope (Fig. 3a). Cytoplasm was mostly condensed, but could contain irregularly shaped vacuoles. Rough endoplasmic reticulum (RER) as well as the Golgi apparatus were not detectable. Accumulations of mitochondria with partially disturbed matrix were prominent and dense bodies were present. The perikarya were surrounded and invaginated by astroglia (Fig. 3a).

Dendrites exhibited basically the same features of degeneration: condensation of dendroplasm (Fig. 3b, c), and accumulation of often enlarged mito-

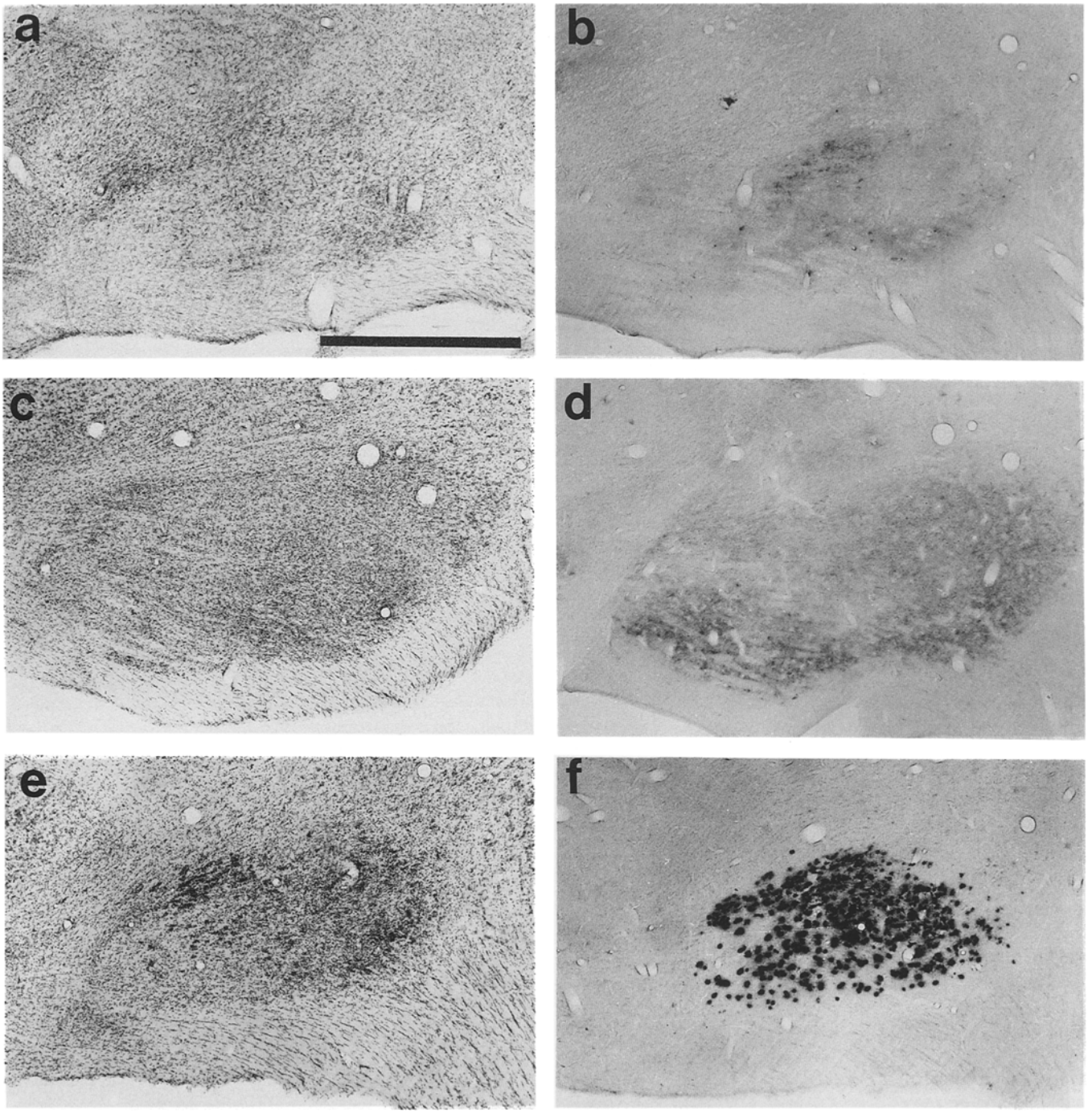

Fig. 1. Sagittal sections through rat substantia nigra (SN) after ibotenic acid (IBO) injection, stained for cresyl violet (**a,c,e**) or Alizarin red (**b,d,f**). **a,b** Four days survival. Neuronal cell loss in whole extent of SN is accompanied by a homogenous to fine-grained Alizarin stain, confined to the SN area. **c,d** Six days survival. Massive astrogliosis in lesioned SN is paralleled by an intense Alizarin red stain which starts to concentrate to small bodies in the anterior-basal parts of SN. **e,f** Four weeks survival. Prominent calcium deposits occupy whole extent of SN and can now be depicted as basophilic bodies in the cresyl stain. *Bar* = 1 mm applies for all micrographs

chondria (Figs. 3c, 4). The surfaces of the dendrites were covered by intact boutons (Figs. 3b, c; 4a), although an occasional local bouton, probably of intrinsic origin, was also seen to degenerate (Figs. 3c, 4a, 5e). A quite characteristic feature was the invagination by astroglial processes into the larger dendrites and their subsequent sequestration (Fig. 4a, c). In rare cases, microglia served the same purpose (Fig. 4b).

The potassium bichromate stain as applied by us did not stain the tissue of control rats or tissue outside the lesioned field of the SN (not shown). Thus, with this technique, physiological Ca^{2+} concentrations would not

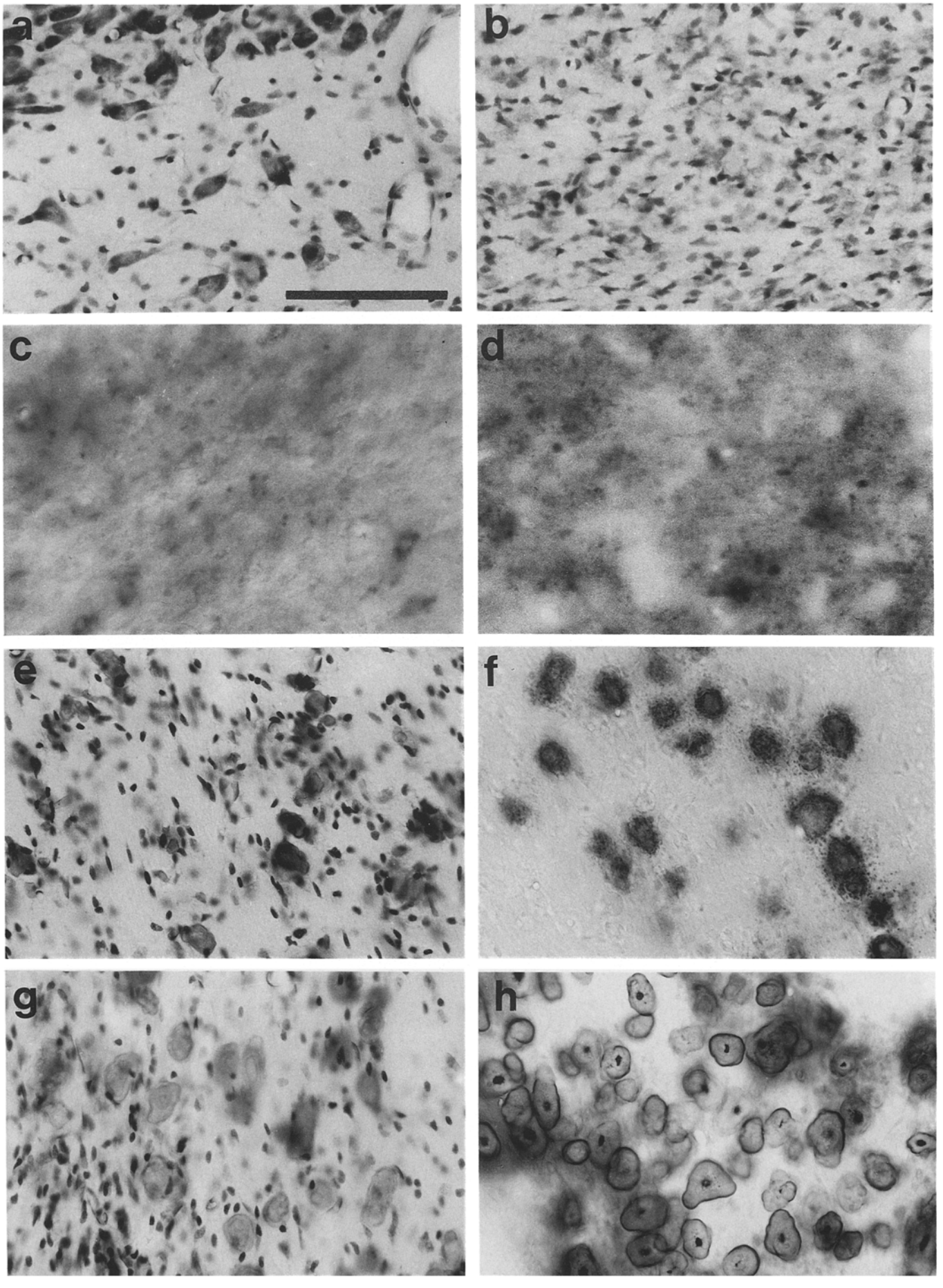
a
b
c
d
e
f
g
h

be detected, rather only pathological accumulations of Ca^{2+} would be visualized.

Two days after IBO application single mitochondria with the electron-dense reaction product of potassium bichromate were found in degenerating neurons (Fig. 3a) and dendrites (Figs. 3c, 4a). It should, however, be noted that by far not all of the degenerating neuronal elements exhibited organelles with an increased Ca^{2+} signal. In particular, they were not found in degenerating boutons (Figs. 3c, 4a).

Four days after IBO injection, the number of Ca^{2+}-containing organelles, mostly identified as mitochondria in dendrites and neuronal somata, was greatly increased (Fig. 4). In addition, single, small dendrites exhibited electron-dense reaction product free in their cytoplasm, i.e. not associated with organelles (Fig. 5a).

Six days after IBO-mediated nerve cell death numerous small dendrites (Fig. 5b) as well as larger ones (Fig. 6) exhibited an increased Ca^{2+} content both in their mitochondria and free in the dendroplasm. In some cases the fine needles of the reaction product were situated in a floccular to fibrillar matrix (dD_1 in Fig. 6). Similar bodies with floccular matrix and Ca^{2+} stain (often with a mitochondrion in the center) were found completely engulfed by astroglia and separated from vacated boutons (Fig. 5d). In one case, an EGTA-treated section, such a body, now without Ca^{2+} stain, was found which still possessed a synaptic contact with a bouton (Fig. 5c). In the direct vicinity of the Ca^{2+}-accumulating dendritic remnants, degenerating dendrites and boutons were present without any pathological Ca^{2+} signal (Fig. 5e). Increased Ca^{2+} was never found in traversing myelinated or unmyelianted axons, nor in astroglia or microglia.

By 2–8 weeks after IBO application the picture had completely changed. Characteristic degenerating elements were no longer observed. Bundles of traversing axons were in good shape but intact boutons were rare. Instead, large conglomerates surrounded by astroglia and/or microglia were seen (Figs. 7–9). In the center of these bodies, remnants of neuronal material were found: mitochondria, membrane whorls, dense bodies, lysosome-like material, and occasionally also neuronal nuclei with parts of their perikaryon as exemplified in Fig. 9a for 8 weeks survival.

The Ca^{2+} stain of the neuronal debris itself was moderate, but it was surrounded by a rim of intense electron-dense material. This was especially evident in the case of the frequent vacuoles (Figs. 7a, 8b). External to the debris floccular to fibrillar material was found which contained a moderate uneven density of Ca^{2+} precipitate. Both the fibrillar matrix and the Ca^{2+} deposition seemed to develop stepwise. After 2 weeks, 1 to 3 rings were seen (Fig. 7a). During the following weeks, more material was added: at 4 weeks survival 8 (Fig. 8a) to 15 rings could be counted. This alternation of layers of low and high electron density resembled the annual growth rings of trees. In cases where the outer perimeter of the concretions was sectioned a nearly evenly dense Ca^{2+} precipitate was seen over the whole structure (Fig. 9b, c). In most cross-sectioned cases, however, the staining was most intense on the outer surface (Fig. 9a). Pretreatment of the sections with EGTA which preferentially removes free Ca^{2+} [47, 50] resulted in a nearly complete loss of the fine electron-dense neddle-shaped material in the vacuoles (Fig. 8c) and the growth rings (Fig. 9d) of the deposits.

In addition to fibrillar materials which was continuously added, together with calcium, in a concentric way to the bodies, the bodies also appeared to participate in the growth, as shown by the formation of coral-shaped protrusions (Fig. 8b, c). These protrusions often ex-

Fig. 2a–h. Histological analysis of SN various times after IBO lesion. **a** SN contralateral to the lesioned side shows in cresyl stain the characteristic densely packed neurons of pars compacta contrasting with the dispersed nerve cells of the pars reticulata. Note also normal density of glial cells and compare with **b**. **b** SN 6 days after IBO injection in cresyl stain. Neurons of pars compacta and pars reticulata have disappeared, gliosis is massive. **c** Four days after IBO application. Alizarin red stains the lesioned area relatively homogenously. Single grains of higher intensity can be recognized. In addition, single cells exhibit stain in their cytoplasm. **d** Six days after IBO application. Alizarin red stain increased in intensity. Accumulation of single grains to larger deposits can be observed. **e** Four weeks after IBO injection, basophilic deposits are clearly visible in cresyl stain. Probably due to the fusion of neighboring particles some of them have a multilobulated cauliflower-like shape. **f** Parallel section to **e**, stained with Alizarin red. Next to the large calcium deposits smaller grains are situated which are not yet incorporated in the concretions. **g** Eight weeks after IBO injection the basophilic bodies have obtained their mature appearance: round to ovoid, multilayered, occasionally multilobulated. Astrogliosis has subsided. **h** Parallel section to **g**, stained with Alizarin red. Smaller grains have disappeared, probably by incorporation in the large concretions. *Bar* = 100 μm applies for all micrographs

Fig. 3a–c. SN, 2 days after local IBO injection, treated with potassium bichromate. **a** Degenerating neuronal perikaryon (*dN*) with condensed chromatin, disintegrated nuclear envelope, vacuoles, dense bodies and accumulation of partially damaged mitochondria. A few of the mitochondria exhibit Ca^{2+} reaction product (*white asterisk*). The neuron is engulfed by reactive astroglia (*Ag*). **b** A degenerating dendrite (*dD*), contacted by morphologically intact boutons (*B*), is surrounded by astroglia (*Ag*). Microglial processes (*Mg*) invade the field. **c** besides degenerated masses (*d*) completely engulfed by astroglia (*Ag*), whose previous identity cannot be discerned, two degenerated dendrites (*dD*), contacted by intact boutons (*B*) are present. The central dD contains an organelle completely filled with potassium bichromate reaction product (*white asterisk*). A few degenerating boutons, identified by their synaptic contacts (*arrowhead*), do not contain Ca^{2+} in visible quantities. Note also that mitochondria of intact boutons, traversing axons and microglia are free of reaction product. *Bars* **a–c** = 1 μm

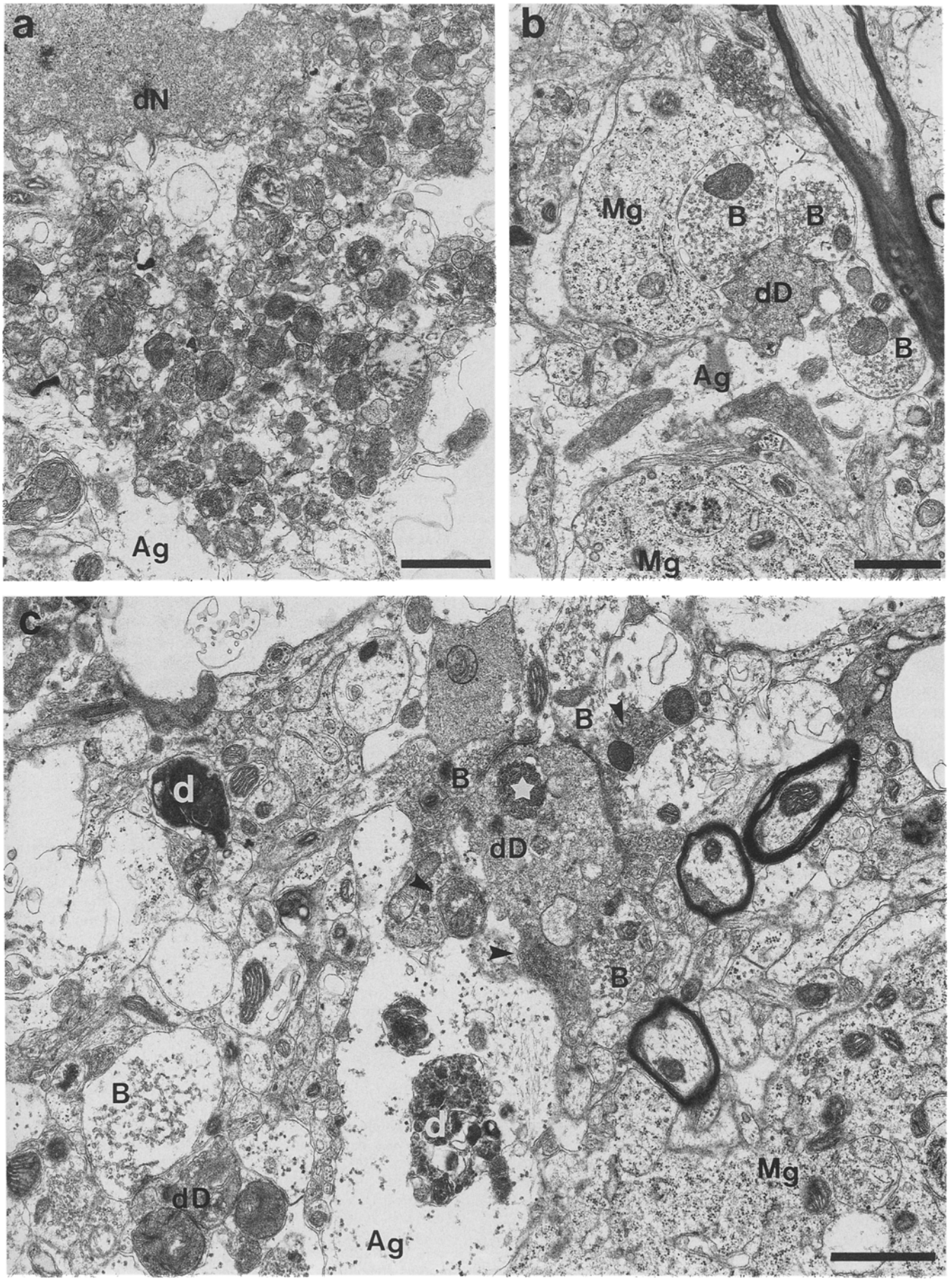

Fig. 3a–c.

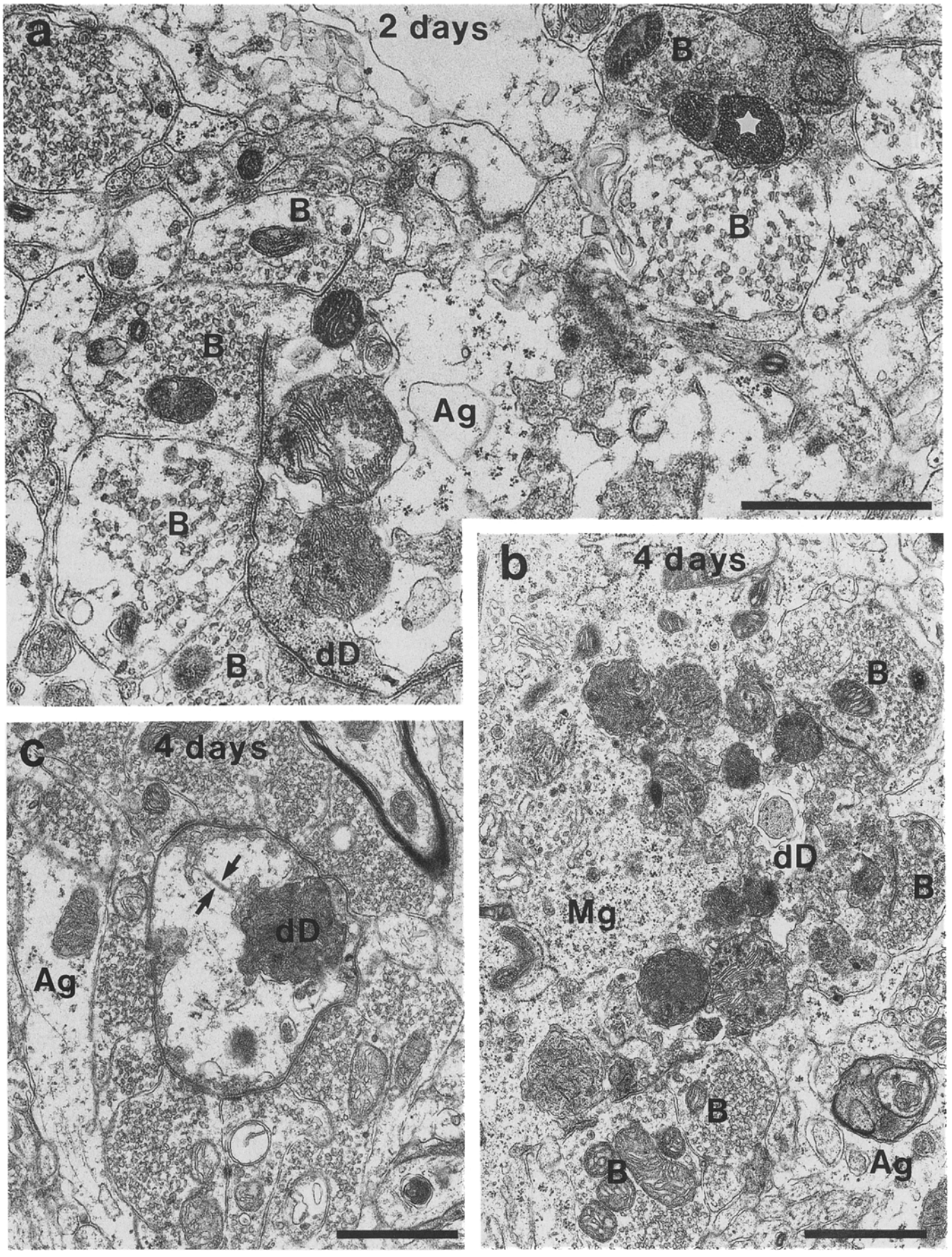

Fig. 4a–c. (for legend see next page)

hibited a matrix-free center with a high density of Ca^{2+} reaction product. Thus, they resembled the vacuoles in the mature concretions. It is, therefore, possible that these protrusions are not so much metastases of a large primary deposit, but rather that growing deposits incorporate smaller degenerated Ca^{2+}-containing materials (e.g., Fig. 8b).

Local IBO application also caused peculiar vascular reactions, not previously described to our knowledge after excitotoxin lesions. They consisted of shrinkage of the capillary endothelium, resulting in vessel luminal diameter much smaller than 7 μm (Fig. 7c), of bizarre networks of basal laminae which penetrated between astroglial and microglial cells towards the neuropil (Fig. 7c), and of perivascular glia which exhibited large interconnected cavities filled with a floccular matrix (Fig. 7d). The outer membrane of these cavities was covered by electron-dense granular material which could potentially represent ribosomes, suggesting that these structures represent swollen RER.

Discussion

In the present study we tried to elucidate the formation of calcium deposits in IBO-lesioned SN observed previously at the light microscopical level 4 weeks after the excitotoxin lesion. For this endeavor we started our investigation with short survival times to determine possible early differences in the exitotoxin-induced degeneration in the SN as compared to the results of other investigators. However, routine light and electron microscopy showed no obvious differences: within 2 days of IBO application neuronal perikarya were either undetectable or showed sign of degeneration in the cresyl stain, as demonstrated by Schwarcz et al. [40] and Tanaka et al. [49] in the SN, and by Köhler and Schwarcz [18] in other brain areas. At the ultrastructural level this was paralleled by the presence of dark degenerating neuronal perikarya and dendrites and dissolution of cytoplasmic organelles, together with well-preserved axons and axon terminals. Similar ultrastructural studies have not yet been carried out in the SN, but observations in IBO-injected CP [43], in KA-injected CP [8, 12], and in KA- or NMDA-infused spinal cord [13, 26] provide results identical to ours, as do the investigations in the hippocampus after systemic KA [44, 47] or domoic acid [46]. A possible difference concerns the glial reaction, in particular the massive infiltration and sequestration of perikarya and dendrites in the presence of still intact surface plasmalemma covered with preserved boutons. However, astroglial reaction of similar distribution and intensity has been described, among other things, during retrograde degeneration in the thalamus [4], in the deafferented vestibular nucleus [17] and, particularly well illustrated after 3-acetylpyridine intoxication in the inferior olive [3]. Thus, the astroglial reaction observed by us is surely not unique for the toxin, IBO, or for the brain area, SN, although a certain region-specific variability in the response to an injury [4] cannot and should not be excluded.

Massive swelling of perivascular glia has been demonstrated by Lassmann et al. [20] in the hippocampus and entorhinal cortex 3 h to 2 days after systemic KA injection, which occasionally resulted in collapsed capillaries with only a slit-like lumen. Our ultrastructural observations show that capillaries with reduced luminal diameter may persist in an excitotoxically lesioned area for more than 2 weeks. In addition, perivascular glia themselves are altered, as evidenced by the massive swelling of RER. Together, these changes seem to affect the extracellular matrix in that the basement membranes lose their defined orientation. These vascular changes could represent endothelial proliferation. According to the older neuropathology literature vascular sprouts are found at the border of ischemic necrotic infarcts [45].

Visualization of Ca^{2+} accumulation after systemic KA has been mostly carried out under the viewpoint of epileptic brain damage and, thus, has been restricted to the first few hours after injection [10, 47, 48]. In these studies, the oxalate-pyroantimonate technique was used in such a sensitivity that the localization of Ca^{2+} in the control preparations was also revealed. A seizure-induced accumulation of Ca^{2+} above control level was mainly found in mitochondria of neuronal perikarya and dendrites and occasionally not associated with a particular organelle in dendrites [10, 47, 48]. However, caution should be taken when comparing seizure-induced Ca^{2+} accumulation with degeneration-induced calcium deposits. The former process is reversible for cells surviving the insult [10, 11], only degenerating neurons retain Ca^{2+} in perikaryal vacuoles [11], thus imitating the situation after transient ischemia [42].

Interestingly, a quantitative analysis of changes in Ca^{2+} content after KA-induced seizures showed continuous increases over the 2- to 4-h value towards the highest concentrations at 7 days [48]. This observation was not paralled by morphological analysis. It would be important to know whether also in this model, the Ca^{2+}

Fig. 4a–c. Degenerating dendrites 2 and 4 days after IBO application in SN. Potassium bichromate stain. **a** Intact presynaptic boutons (*B*) demarcate the contours of a degenerating dendrite (*dD*) which has been invaginated by astroglial processes (*Ag*), as suggested by the presence of glycogen. A small dendrite in the *upper right corner,* contacted by two intact boutons (*B*) and a degenerated one is extremely shrunken. It contains two membrane-covered bodies filled with precipitate (*white asterisk*). **b** Only the left perimeter of a former large dendrite (*dD*) can be recognized due to the presence of synaptic contacts with intact boutons (*B*). From the left microglia (*Mg*) has invaded the neuronal structure. Some of the disintegrated dendritic mitochondria exhibit potassium bichromate stain. *Ag,* Astroglia. **c** The previous outline of a dendrite can be recognized by the position of the intact synaptic contacts which are in most parts covered with a thin rim of condensed dendroplasm and a larger accumulation of mitochondria (*dD*). Astroglia lamellae (*Ag*) characterized by glial filaments and glycogen have invaded the former dendrite and form there a gap junction (*opposing arrows*). *Bars* **a–c** = 1 μm

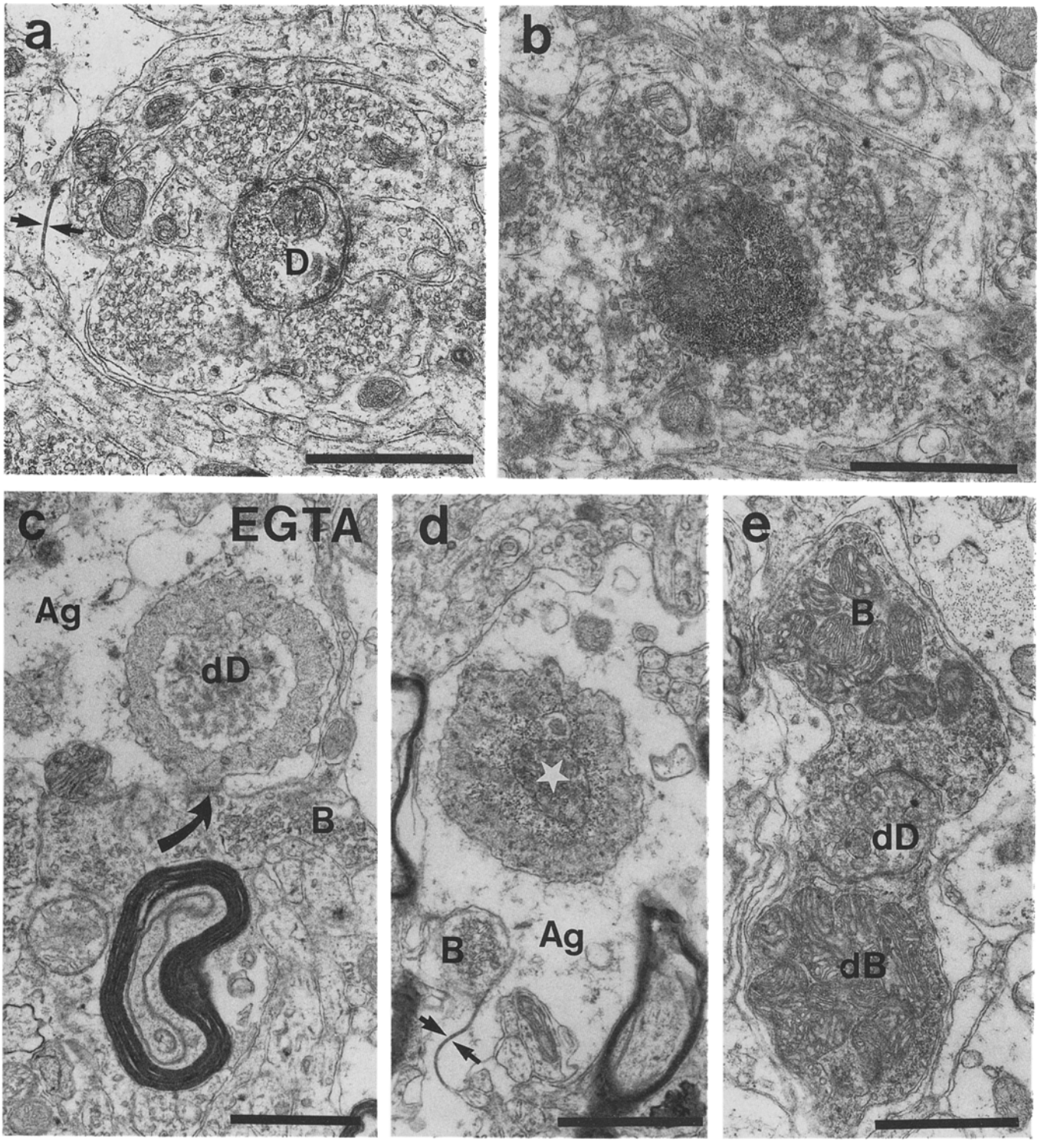

Fig. 5. IBO induced changes of peripheral dendrites in SN 4 days (**a**) and 6 days (**b**–**e**) after application of the toxin. Potassium bichromate stain. **a** Vibratome section treated with potassium bichromate exhibits electron-dense precipitate in the dendroplasm (*D*) and in the mitochondrion. The plasmalemma of the dendrite is preserved, contacted by intact boutons. Astroglial sheets connected by gap junction (*opposing arrows*) only cover the complex in the periphery of the boutons. **b** Comparable dendrite processed as in **a** shows 2 days later an increased accumulation of dense precipitate. The plasmalemma is irregular but still contacted by intact boutons. **c** Vibratome section pretreated with the Ca^{2+}-chelator EGTA. An object, comparable in size and appearance to that shown in **d**, but lacking the elctron-dense precipitate, is nearly completely engulfed by astroglia (*Ag*). Only a small contact zone with a bouton (*B*) is preserved, suggesting that this structure has been a dendrite. **d** A roundish object with a mitochondria-like structure in the center exhibits some electron-dense reaction product in a floccular matrix (*white asterisk*). It is completely engulfed by astroglial extensions (*Ag*) which are joined by gap junctions (*opposing arrows*). The astroglia separates the particle from bundles of unmyelinated axons and from an isolated bouton (*B*). **e** In the direct neighborhood of **d** a degenerating dendrite (*dD*) is found without any Ca^{2+} precipitate. It is contacted by an intact bouton (*B*) and a degenerating one (*dB*), as evidenced by the dark synaptoplasm and the aggregation of enlarged mitochondria. *Bars* **a**–**e** = 1 μm

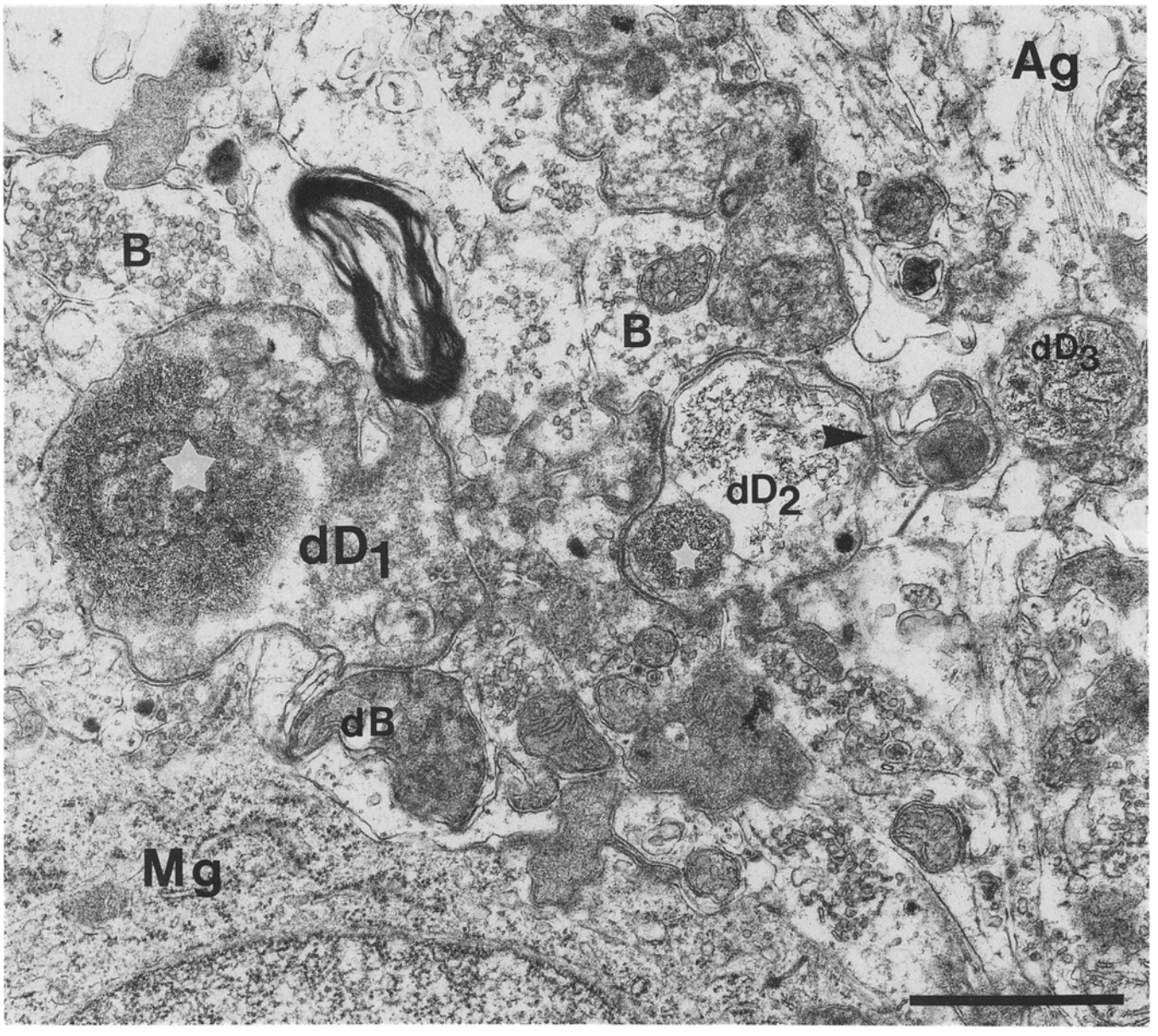

Fig. 6. SN 6 days after local IBO application. Potassium bichromate stain. In a large dendrite (dD_1), still discernible by the plasmalemma intensified by synaptic contact zones with an intact (*B*) and a degenerating bouton (*dB*), an electron-dense precipitate is found in the remnant of the mitochondrion (*white asterisk*) and accumulated in its vicinity. The remainder of the dendrite is filled by condensed, floccular material. A smaller electron-lucent dendrite (dD_2) which is in synaptic contact with a degenerating bouton (*arrowhead*) contains the Ca^{2+} stain free in the cytoplasm as well as concentrated in a rounded organelle (*asterisk*). A third Ca^{2+} aggregation (dD_3) is completely engulfed by astroglia (*Ag*). *Bar* = 1 μm

Fig. 7a–d. SN 2 weeks after local IBO application. Potassium bichromate stain. **a** Neuronal cellular debris, which occasionally can be identified as mitochondria and vacuoles with Ca^{2+} stain at the membrane, is embedded in a floccular matrix. The layered, onion-shaped structure of the deposits, resembling the growth rings of trees, can be recognized. Ca^{2+} stain is most intense at the border zones to the next layer. **b** Vibratome section pretreated with EGTA. A large amorphous deposit containing mitochondria, dense bodies and membrane whorls possesses at its surface fibrillar to floccular material, possibly one of the focuses for Ca^{2+} accumulation. It is surrounded by macrophages (*Mg*). **c** The thick endothelium of a capillary with enlarged nucleus leaves only a narrow lumen of 3-μm diameter. The endothelium is covered by a complex net of basal lamina (*arrows*). They are in turn only partially covered with astroglia (*Ag*); microglia (*Mg*) also border the basal lamina of the vessel. **d** A large diameter capillary is engulfed nearly in its whole circumference by an astrocyte (*Ag*), which exhibits interconnected compartments, the membranes towards the cytoplasm covered with a dense precipitate. *d*, Degenerated dense masses covered with microglia. *Bars* **a–d** = 1 μm

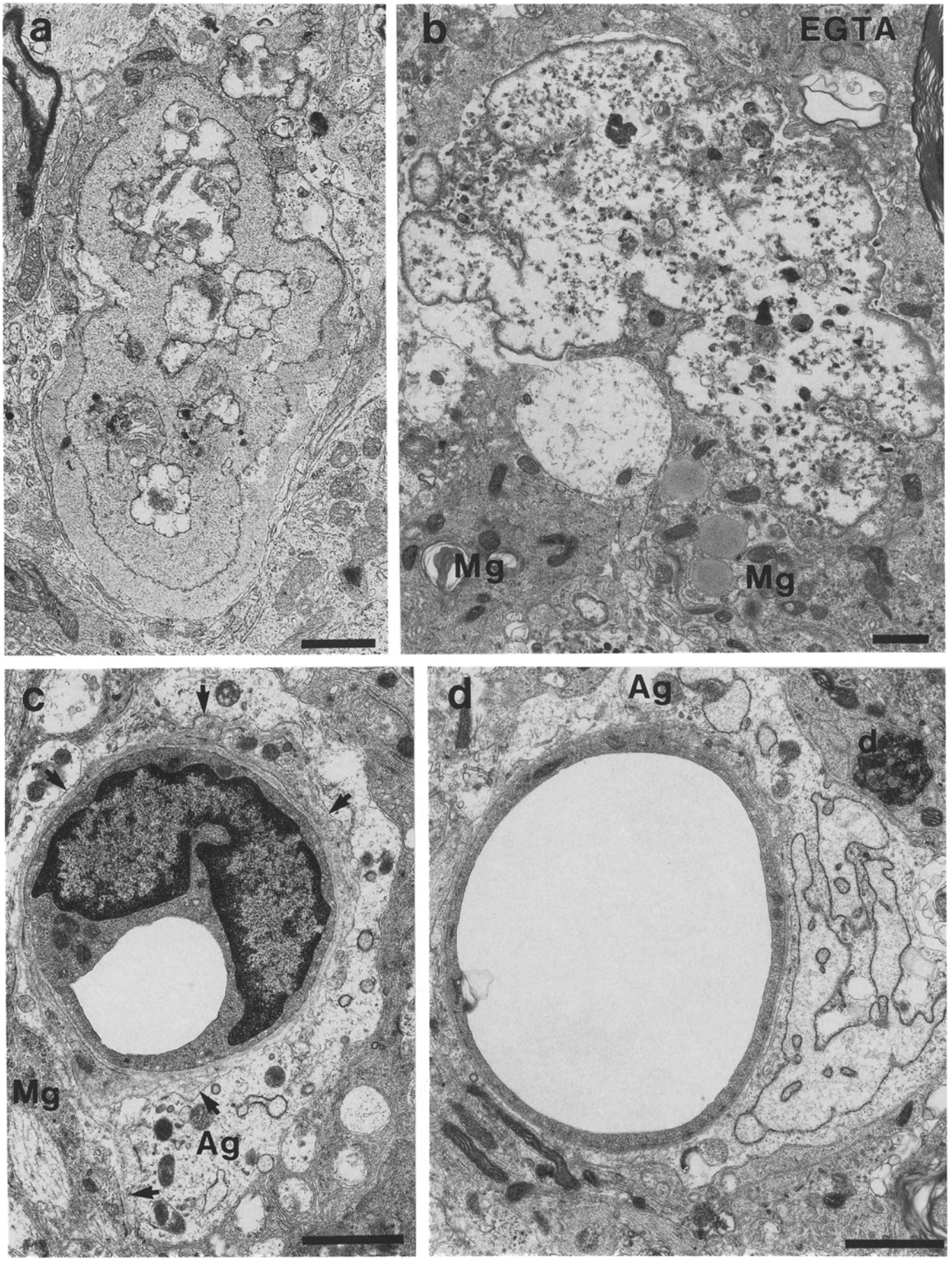
a
b
EGTA
Mg
Mg
c
Mg
Ag
d
Ag
d

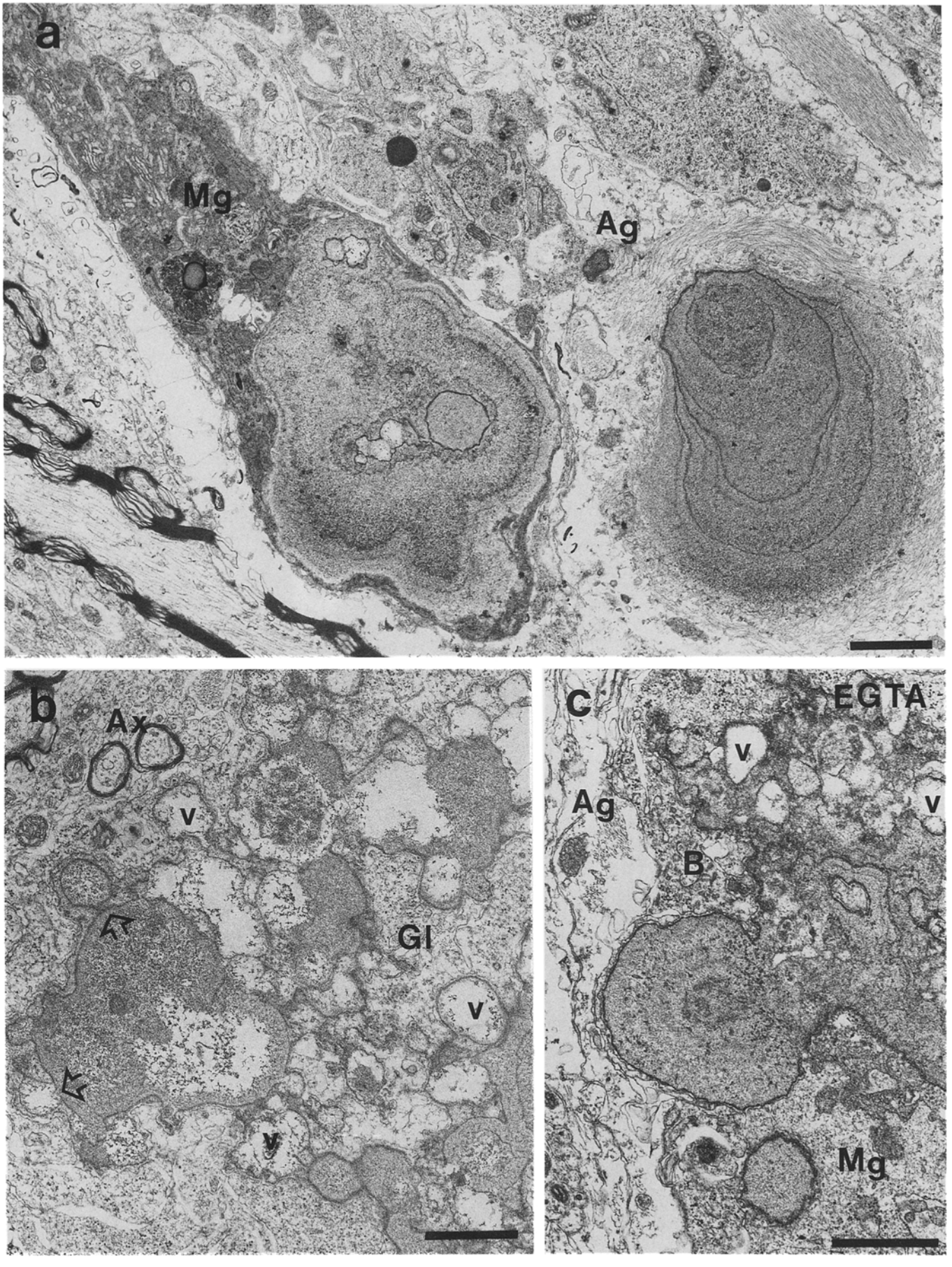
a
Mg
Ag
b
Ax
v
Gl
v
v
v
C
EGTA
v
Ag
v
B
Mg

accumulation is most prominent between days 4 and 6 and whether this is associated with organelles or in a seemingly free form in the dendroplasm (see Fig. 6). Whether the excessive Ca^{2+} accumulation is now the signal for the astroglia to engulf the dendrite and to separate it from its remaining boutons (compare Fig. 5b, c and d) is still a matter of speculation.

In any case, the present ultrastructural findings strongly suggest that at the border of the primary accumulation of seemingly free calcium and the surrounding glia, a fibrillar matrix is formed which is able to further accumulate calcium. From studies of calcification processes, be it on the basis of necrotic tissue damage or the age-related formation of concretions in the pineal gland, it is generally accepted that the matrix consists of acid mucopolysaccharides complexed to a protein [1, 5, 14, 16]. The source for these matrix components is still completely open for speculation. Based on studies from cerebral artherosclerosis it has generally been taken for granted that the initial process starts in blood vessels which deposit acid mucopolysaccharides in the outer layer of the vessels and in perivascular tissue [1, 27]. Also, macrophages activated by inflammation or by release of free radicals during neuronal degeneration can produce a mucopolysaccharide matrix [5, 21]. In fact, calcification in basal ganglia is found in autoimmune diseases [31] and inflammatory conditions of the brain [25]. Extracellular matrix proteins could provide the glycoproteins postulated to be a component of the fibrillar matrix of the calcium concretions [33]. The continuously enlarging concretions are then obviously able to incorporate smaller deposits, thereby forming bodies of considerable size. Thus, the crucial event for the generation of microscopically detectable growing concretions seems to be the ever-enlarging formation of a matrix which allows the deposition of calcium. Surely, in a next step the constituents of this matrix must be analyzed.

How is it possible that this IBO-induced calcification has not been observed beforehand? One reason might be that prominent deposits are found at the ultrastructural level only after 2 weeks, and at the histological level in routine stain only after 4 to 8 weeks. IBO injections in the SN with longer survival periods have not yet been carried out. Injections with KA in the SN with survivals of 3 months did not show any histological pecularity [36], and the same was the case with IBO injection in the CP with survivals of 60 days [43], 4 months [32] and 6 months [15]. Our own investigation on Ca^{2+} accumulation visualized with Alizarin red stain in IBO-injected CP also showed that, although calcium signal increases in a few cases, formation of deposits does not occur [28]. From this it can tentatively be concluded that both the nature of the toxin as well as structural and metabolic pecularities of the brain region determine whether or not calcification will take place.

The toxin, IBO, was for a long time considered as a relatively specific agonist of the NMDA type of the glutamate receptor which gates a Ca^{2+} channel [9, 51]. Recent evidence, however, indicates that IBO is in addition a powerful agonist at the metabotropic glutamate receptor. This receptor is directly coupled to a second messenger cascade which, via inositol 1, 4, 5-triphosphate, mediates the release of Ca^{2+} from intracellular stores [6]. Thus, accumulation of free Ca^{2+} in dendroplasm could proceed via two sources: extracellular via NMDA- and voltage-gated Ca^{2+} channels and from intracellular stores. In this context it is noteworthy that astrocytes also possess a metabotropic glutamate receptor [2]. The regional distribution of NMDA receptors is different from brain region to brain region – it is comparably low in the SN [24] – and surely the metabotropic glutamate receptor is also unevenly distributed. Of course, regional differences only mirror in part differences at the cellular level: different receptor outfits of neuronal and glial subpopulations. Thus, it is quite possible that distinct intrinsic factors in the SN, be it the neuronal and glial outfit with various glutamate receptors, or the response repertoire of astro- and microglial cells to the injury, provide the molecular basis for the formation of calcium deposits.

The conditions under which brain calcification is observed in human patients have been reviewed, among others by Adachi et al. [1] and Beall et al. [5]. The idiopathic calcification, Fahr's disease, is bilateral and shows a certain predilection for the cerebellar dentate nucleus, the basal ganglia, and the globus pallidus, in

Fig. 8a–c. SN 4 weeks after local IBO application, potassium bichromate stain. **a** Two large bodies exhibit Ca^{2+} precipitate in layers of varying densities in a floccular matrix accumulated around cellular debris in the center. The profiles are engulfed by microglia (*Mg*) or astroglia (*Ag*). **b** Multilobulated Ca^{2+} deposits with high Ca^{2+} signal in their matrix-free centers and in vacuoles (*v*) are surrounded and invaginated by glial processes (*Gl*). Tiny coral-shaped profiles (*open arrows*) seem to bud off from (or fuse with) the main body. Note preserved bundle of myelinated and unmyelinated fibers (*Ax*). **c** Treatment of the section with EGTA completely abolishes the Ca^{2+} stain in the matrix-filled and in the matrix-free areas of the body and in the vacuoles (*v*). The onion-layered coral-shaped protrusion has contact with a bouton (*B*). Elsewhere the body is covered by astroglia (*Ag*) or microglia (*Mg*). *Bars* **a–c** = 1 μm

Fig. 9a–d. Ca^{2+} deposits 8 weeks after IBO injection. Potassium bichromate stain. **a** In the center of this deposit, remnants of a neuronal perikaryon (nucleus, mitochondria, dense bodies) are found in a fibrillar matrix infiltrated to a varying degree with Ca^{2+} precipitate. Toward the surface the highest density of Ca^{2+} stain is found. **b** High magnification (see *bar* in **d**) of the surface area of a huge deposit densely infiltrated with Ca^{2+} precipitate. **c** Round body whose fibrillar matrix is intensely covered with Ca^{2+} stain. **d** Removal of Ca^{2+} by EGTA allows the visualization of the floccular to fibrillar matrix of the mature concrements. *Bars* **a,c,d** = 1 μm

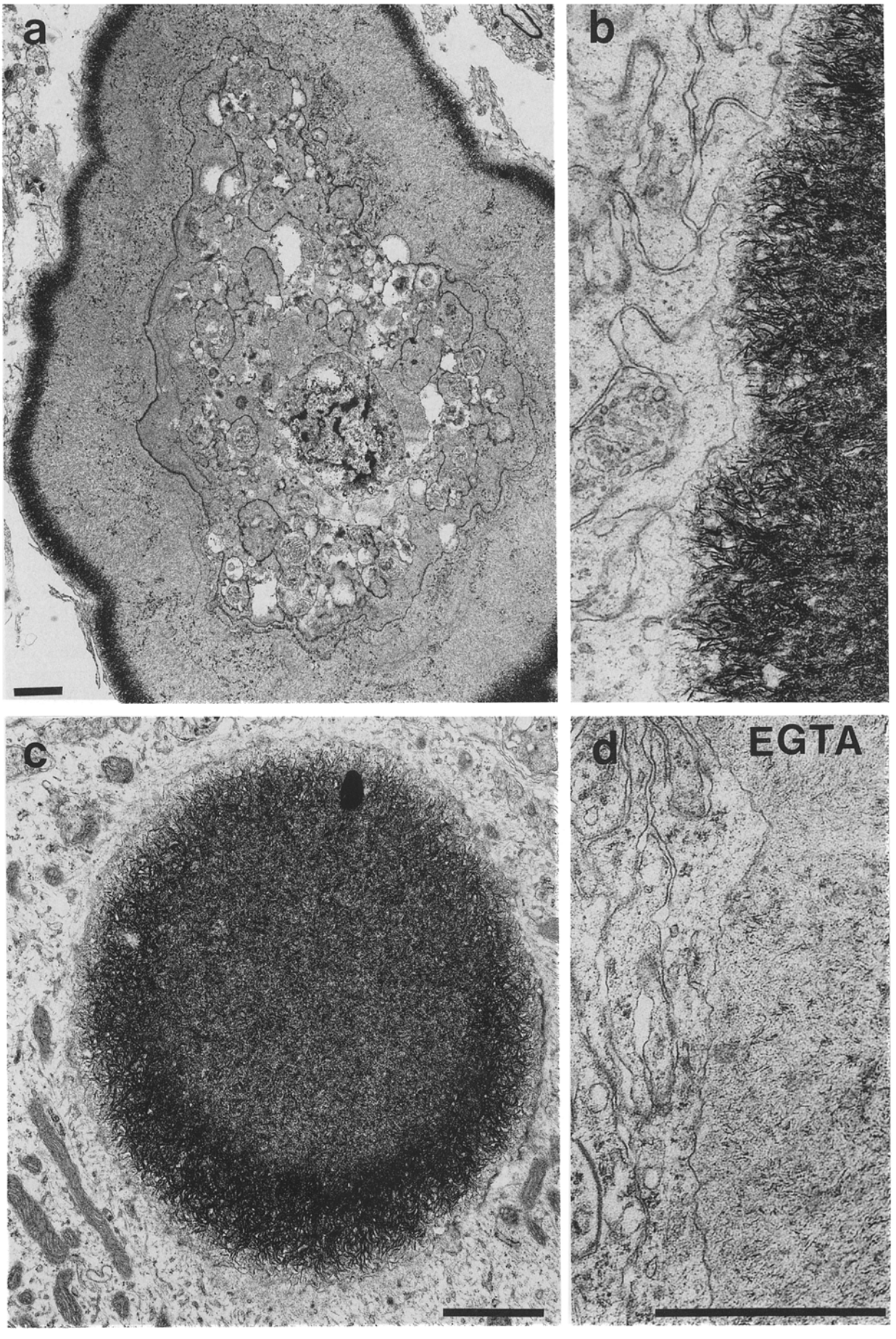

Fig. 9a–d.

particular [1]. It is not known, but worth to be considered, whether this calcification process occurs on the basis of an excitotoxic neurodegenerative event. In any case, the highly reliable IBO-induced calcification in the SN can serve as a model to study the molecular basis of non-arteriosclerotic calcification.

Acknowledgements. We thank Mr. H. Stöcklin for expert photographic work and Ms. D. Müller for secretarial help.

References

1. Adachi M, Wellmann KF, Volk BW (1968) Histochemical studies on the pathogenesis of idiopathic non-arteriosclereotic cerebral calcification. J Neuropathol Exp Neurol 27:483–499
2. Ahmed Z, Lewis CA, Faber DS (1990) Glutamate stimulates release of Ca^{2+} from internal stores in astroglia. Brain Res 516:165–169
3. Anderson WA, Flumerfelt BA (1980) A light and electron microscopic study of the effects of 3-acetylpyridine intoxication on the inferior olivary complex and cerebellar cortex. J Comp Neurol 190:157–174
4. Barron KD, Means ED, Larsen E (1973) Ultrastructure of retrograde degeneration in thalamus of rat. J Neuropathol Exp Neurol 32:218–244
5. Beall SS, Patten BM, Mallette L, Jankovic J (1989) Abnormal systemic metabolism of iron, porphyrin, and calcium in Fahr's syndrome. Ann Neurol 26:569–575
6. Collingridge GL, Lester RAJ (1989) Excitatory amino acid receptors in the vertebrate central nervous system. Pharmacol Rev 40:143–210
7. Coyle JT (1983) Neurotoxic action of kainic acid. J Neurochem 41:1–11
8. Coyle JT, Molliver ME, Kuhar MJ (1978) In situ injection of kainic acid: a new method for selectively lesioning neuronal cell bodies while sparing axons of passage. J Comp Neurol 180:301–323
9. Curtis DR, Lodge D, McLennan H (1979) The excitation and depression of spinal neurons by ibotenic acid. J Physiol (Lond) 291:19–28
10. Evans MC, Griffiths T, Meldrum BS (1984) Kainic acid seizures and the reversibility of calcium loading in vulnerable neurons in the hippocampus. Neuropathol Appl Neurobiol 10:285–302
11. Griffiths T, Evans MC, Meldrum BS (1984) Status epilepticus: the reversibility of calcium loading and acute neuronal pathological changes in the rat hippocampus. Neuroscience 12:557–567
12. Hattori T, McGeer EG (1977) Fine structural changes in the rat striatum after local injections of kainic acid. Brain Res 129:174–180
13. Hugon J, Vallat JM, Spencer PS, Leboutet MJ, Barthe D (1989) Kainic acid induces early and delayed degenerative neuronal changes in rat spinal cord. Neurosci Lett 104:258–262
14. Humbert W, Pévet P (1991) Calcium content and concretions of pineal glands of young and old rats. Cell Tissue Res 263:593–596
15. Isacson O, Fischer W, Wictorin K, Dawbarn D, Björklund A (1987) Astroglial response in the excitotoxically lesioned neostriatum and its projection areas in the rat. Neuroscience 20:1043–1056
16. Japha JL, Eder TJ, Goldsmith EG (1976) Calcified inclusions in the superficial pineal gland of the Mongolian gerbil, *Meriones unguiculatus*. Acta Anat (Basel) 94:533–544
17. Johnson JE Jr. (1975) An fine structural study of degenerative-regenerative pathology in the surgically deafferentated lateral vestibular nucleus of the rat. Acta Neuropathol (Berl) 33:227–243
18. Köhler C, Schwarcz R (1983) Comparison of ibotenate and kainate neurotoxicity in rat brain: a histological study. Neuroscience 8:819–835
19. Komulainen H, Bondy SC (1988) Increased free intracellular Ca^{2+} by toxic agents: an index of potential neurotoxicity? Trends Pharmacol Sci 9:154–156
20. Lassmann H, Petsche U, Kitz K, Baran H, Sperk G, Seitelberger F, Hornykiewicz O (1984) The role of brain edema in epileptic brain damage induced by systemic kainic acid injection. Neuroscience 13:691–704
21. Löwenthal A, Bruyn GW (1968) Calcification of striopallidodentate system. In: Vinken PJ, Bruyn GW (eds) Handbook of clinical neurology. Elsevier, New York, pp 703–709
22. MacDermott AB, Mayer ML, Westbrook GL, Smith SJ, Barker JL (1986) NMDA-receptor activation increases cytoplasmic calcium concentration in cultured spinal cord neurones. Nature 321:519–522
23. Mayer ML, Westbrook GL (1987) The physiology of excitatory amino acids in the vertebrate central nervous system. Prog Neurobiol 28:197–276
24. Monaghan DT, Cotman CW (1985) Distribution of *N*-methyl-D-aspartate-sensitive L-[^{3}H]glutamate-binding sites in rat brain. J Neurosci 5:2909–2919
25. Morgante L, Vita G, Meduri M (1986) Fahr's syndrome: local inflammatory factors in the pathogenesis of calcification. J Neurol 233: 19–22
26. Nag S, Riopelle RJ (1990) Spinal neuronal pathology associated with continuous intrathecal infusion of *N*-methyl-D-aspartate in the rat. Acta Neuropathol 81:7–13
27. Neumann MA (1963) Iron and calcium dysmetabolism in the brain. J Neuropathol Exp Neurol 22:148–163
28. Nitsch C, Schaefer F (1990) Calcium deposits develop in rat substantia nigra but not striatum several weeks after local ibotenic acid injection. Brain Res Bull 25:769–773
29. Nitsch C, Schaefer F, Scotti AL (1991) Ibotenic acid-induced calcium deposits in rat brain: a histochemical light and electron microscopic analysis. Prog Histochem Cytochem 23:243–248
30. Nitsch C, Wolfrum G, Schaefer F, Scotti AL, Unger J (1992) Opposite effects of intranigral ibotenic acid and 6-hydroxydopamine on motor behavior and on striatal neuropeptide Y neurons. Brain Res Bull (in press)
31. Nordstrom DM, West SG, Andersen PA (1985) Basal ganglia calcifications in central nervous system lupus erythematosus. Arthritis Rheum 28:1412–1416
32. Nothias F, Wictorin K, Isacson O, Björklund A, Peschanski M (1988) Morphological alteration of thalamic afferents in the excitotoxically lesioned striatum. Brain Res 461:349–354
33. Palladini G, Alfei L, Appicciutoli L (1965) Histochemical observations concerning the corpora arenaca of human epiphysis. Arch Ital Anat Embriol 70:253–270
34. Paxinos G, Watson C (1986) The rat brain in stereotaxic coordinates, 2nd ed. Academic Press, Sydney
35. Pellegrino LJ, Pellegrino AS, Cushman AJ (1979) A stereotaxic atlas of the rat brain. Plenum Press, New York
36. Pritzel M, Huston JP, Sarter M (1983) Behavioral and neuronal reorganization after unilateral substantia nigra lesions: Evidence for increased interhemispheric nigrostriatal projections. Neuroscience 9:879–888
37. Probst W (1986) Ultrastructural localization of calcium in the CNS of vertebrates. Histochemistry 85:231–239
38. Robinson MB, Coyle JT (1987) Glutamate and related acidic excitatory neurotransmitters: from basic science to clinical application. FASEB J 1:446–455
39. Romeis B (1968) Mikroskopische Technik. Oldenbourg, München
40. Schwarcz R, Hökfelt T, Fuxe K, Jonsson G, Goldstein M, Terenius L (1979) Ibotenic acid-induced neuronal degeneration: a morphological and neurochemical study. Exp Brain Res 37:199–216

41. Schwob JE, Fuller T, Price JL, Olney JW (1980) Widespread patterns of neuronal damage following systemic or intracerebral injections of kainic acid: a histological study. Neuroscience 5:991–1014
42. Simon RP, Griffiths T, Evans MC, Swan JH, Meldrum BS (1984) Calcium overload in selectively vulnerable neurons of the hippocampus during and after ischemia: an electron microscopy study in the rat. J Cereb Blood Flow Metab 4:350–361
43. Smith DE, Saji M, Joh TH, Reis DJ, Pickel VM (1987) Ibotenic acid-induced lesions of striatal target and projection neurons: ultrastructural manifestations in dopaminergic and nondopaminergic neurons and in glia. Histol Histopathol 2:251–263
44. Sperk G, Lassmann H, Baran H, Kish SJ, Seitelberger F, Hornykiewicz O (1983) Kainic acid induced seizures: neurochemical and histopathological changes. Neuroscience 10:1301–1315
45. Spielmeyer W (1922) Histopathologie des Nervensystems. Springer-Verlag, Berlin
46. Strain SM, Tasker RAR (1991) Hippocampal damage produced by systemic injections of domoic acid in mice. Neuroscience 44:343–352
47. Sztriha L, Joó F, Szerdahelyi P (1985) Accumulation of calcium in the rat hippocampus during kainic acid seizures. Brain Res 360:51–57
48. Sztriha L, Joó F, Szerdahelyi P (1986) Time-course of changes in water, sodium, potassium and calcium contents of various brain regions in rats after systemic kainic acid administration. Acta Neuropathol 70:169–176
49. Tanaka T, Tanaka S, Kaijima M, Yonemasu Y (1989) Ibotenic acid-induced nigral lesion and limbic seizure in cats. Brain Res 498:215–220
50. Thomas MV (1983) Techniques in calcium research. Academic Press, London
51. Zorumski CF, Todd RD, Clifford DB (1989) Complex responses activated by ibotenate in postnatal rat hippocampal neurons. Brain Res 494:193–197